

ANALYSIS OF THE ELECTROMAGNETIC FIELD  
IN A CONTROLLED ENCLOSURE FOR BIOLOGICAL  
DOSIMETRY  
PART 1. DESIGN AND VALIDATION OF THE NUMERICAL MODEL

MIHAELA MOREGA<sup>1</sup>, SIMONA MICLĂUȘ<sup>2</sup>, ALINA MACHEDON<sup>1</sup>

**Key words:** FEM analysis of EMF, TEM cell, Microwaves dosimetry.

A numerical and experimental study of the electromagnetic field (EMF) is presented in the paper. It is focused on the investigation of the electric field quality inside a transversal electromagnetic cell (TEM cell), used as a controlled enclosure for biological dosimetry assessment. Inside the cell, the target sample is exposed to EMF in the range of radiofrequency (RF) or microwaves (MW), in conditions that are currently assumed to simulate free-space exposure. The identification and control of some proper exposure conditions are primarily required for the design of the dosimetric experiment. COMSOL Multiphysics is the numerical tool used for finite element (FEM) modeling of the EMF inside the TEM cell. *Part 1* presents the design of the numerical model and its validation, both by experimental and theoretical methods. Some characteristics of the TEM cell are also determined, with the main goal of assessing the uniformity of the electric field in the region where the biological sample is exposed to microwaves. *Part 2* directs the FEM analysis of the model to the evaluation of some dosimetric quantities relative to the exposed biological material and analyses the stability of the exposure conditions at small variations of the EMF frequency.

## 1. INTRODUCTION

Far field exposure of biological material to microwaves is necessary for dosimetric analysis; a proper EMF environment is needed during the study of bioeffects in radiofrequency dosimetry, for a controlled exposure of biologic material. Experimental and numerical techniques, that complement each other in gathering inner field parameters, are useful for biological effects characterization. Experimental work on biological effects due to RF and MW field exposure needs a high quality dosimetric assessment. A relevant statistics of a quantified effect is strictly connected to the same exposure conditions throughout the whole volume of the biological sample. One of the commonly used plane wave exposure devices is the TEM-mode

---

<sup>1</sup> “Politehnica” University of Bucharest, Electrical Engineering Department, E-mail: mihaela@iem.pub.ro

<sup>2</sup> Land Forces Academy Nicolae Balcescu, Sibiu

chamber or TEM cell, which offers the advantages of being versatile in size, relatively inexpensive, and relatively broad-banded. It could be regarded as a coaxial line wherein the inner conductor (septum) is a flat plate and the outer conductor is a rectangular tube. The TEM cell actually consists of a main rectangular waveguide (section used for the experimental dosimetry) continued with adjacent tapered transition sections that adapt the dimensions of the cell to the end ports; usually, one port is connected to the MW source through a coaxial cable and the other connects a matched load impedance [1, 2]. The adequate correlation among exposure parameters is based on several objectives: maximum test volume, maximum MW frequency limit, proper quality of the electric field distribution (maximum uniformity, minimum standing waves, minimum reflections, minimum higher order modes) [3]. We currently use a rectangular TEM cell for the controlled exposure of small volume biological samples, either plant seeds, plant and animal tissues, or even small size animals from inferior species.

Whole body *specific energy absorption rate (SAR)* inside the exposed sample could be measured using simultaneously three power meters, by a differential estimation; the incident power density and polarization effects can also be determined. A network analyzer, connected so as to obtain the reflection and transmission information, provides the scattering parameters (S-parameters) for the unloaded or loaded cell. **E**- and **H**-field maps are required to control the EMF distribution inside the cell, in order to avoid higher order propagation modes and excessive wave reflections at the metallic walls that alter electric field uniformity.

MW penetration depth inside an exposed biological sample is in the order of centimeters, and the inner electric field distribution, required for the dosimetric analysis, is generally non-uniform. On the other hand, direct measurements of the electric field strength and *SAR* at any location inside the exposed biological sample are almost impossible to be performed with adequate accuracy. It becomes necessary to equally use a theoretical approach, in parallel to the experimental analysis, and the numerical modeling is the technique able to provide complementary information to the experiment. A preliminary phase of the dosimetric study should therefore be the design and validation of the numerical model, able to simulate the experimental conditions. The computational model complements data obtained from the experiment and is useful for preparing the test (finding a proper correlation among exposure parameters) as much as for extending the processing of the results.

## 2. NUMERICAL MODEL

The theoretical study focuses on the TEM cell numerical model description and validation, followed by the evaluation of the EMF parameters inside the cell. Most EMF models of TEM cells refer only to the central rectangular part, where a

TEM modal structure or a static field distribution is currently assumed [1, 3]. However, numerical techniques are able to model the entire cell geometry and different working conditions (useful especially when the quality of the electric field is assessed) as, for example, in [2] and [4], where the finite-difference time-domain (FDTD) method is used, or in [5] and [6] where a finite element method (FEM) model is referred.

## 2.1. MODEL DESCRIPTION

The FEM implemented by the commercial COMSOL Multiphysics [7] is used in our work for the generation of the numerical model that simulates the TEM cell (rectangular cell, model IFI CC 104 SEXX) available to us for experimental dosimetry tests. The TEM cell has the geometry and dimensions showed in Fig. 1 and table 1 (middle column). One of the procedures used for the validation of the numerical model is further performed against a set of theoretical results given by Popovic et al. [2]. The geometric characteristics of the model introduced in paper [2] are specified in table 1 (last column).

Table 1

TEM cell dimensions

[mm]	TEM cell model IFI CC 104	TEM cell model in paper [2]
$A$	450	300
$B$	450	80
$C$	450	136
$L$	850	564
$a$	25	21
$b$	25	19
$c$	19	14
$a_1 = a_2$	225	140
$b_1 = b_2$	224	39.5
$b_3$	380	100
$d$	2	1
$d_1 = d_2$	200	132
$g$	35	18

The numerical 3D FEM model is implemented with COMSOL Multiphysics, *RF module* [7]. *Harmonic propagation regime of electromagnetic waves*, solved for  $\mathbf{E}$  in complex numbers representation and *eigen-frequency analysis* were applied for the study presented in the paper. The general wave equation, in terms of electric field strength  $\mathbf{E}$

$$\nabla \times \left( \frac{1}{\mu} \nabla \times \mathbf{E} \right) - \omega^2 \left( \epsilon - j \frac{\sigma}{\omega} \right) \mathbf{E} = 0 \quad (1)$$

is valid for the computational domain enclosed by the TEM cell, where  $\omega = 2\pi f$ ,  $j = \sqrt{-1}$  and  $\mu$ ,  $\epsilon$ ,  $\sigma$  are the magnetic and electric properties of the subdomains.

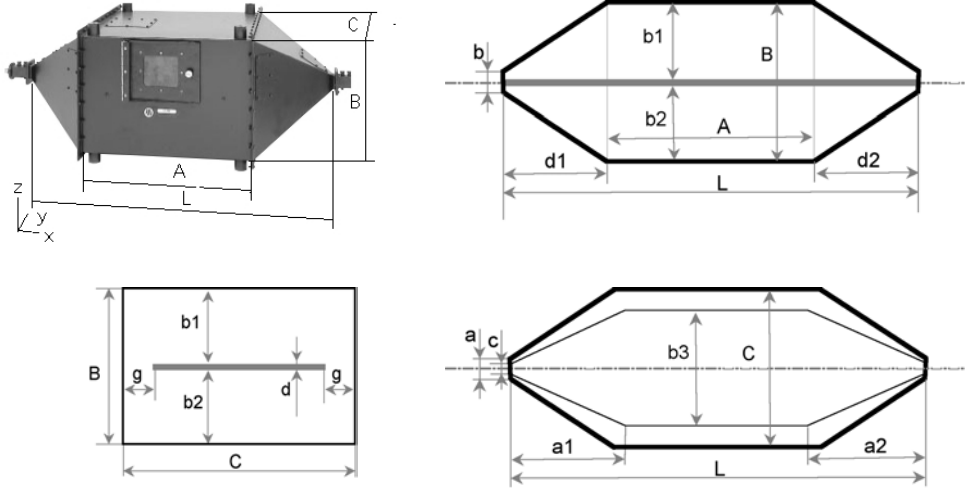


Fig. 1 – The geometry of the TEM cell (according to dimensions in Table 1).

The left end of the TEM cell acts as the radiation source, defined through a *port boundary condition* where the incident  $\mathbf{E}$ -field is introduced according to the TEM mode propagation of the waves in the coaxial cable which connects the MW generator to that port; the software implementation also facilitates the computing of scattering parameters when the port boundary condition is used. The right end is modeled through an *adapted impedance boundary condition*, assuming that no wave reflections occur there and the electric field strength on that surface,  $\mathbf{E}_s$  is specified accordingly

$$\sqrt{\mu}(\mathbf{n} \times \mathbf{H}) + \left( \sqrt{\epsilon - j\frac{\sigma}{\omega}} \right) (\mathbf{n} \times (\mathbf{E} \times \mathbf{n})) = - \left( \sqrt{\epsilon - j\frac{\sigma}{\omega}} \right) (-\mathbf{n} \times (\mathbf{E}_s \times \mathbf{n})). \quad (2)$$

The metallic enclosure and the median conductive septum are considered *perfect electric conductors*

$$\mathbf{n} \times \mathbf{E} = 0. \quad (3)$$

The numerical model may take advantage of *symmetry conditions*, especially when the unloaded cell is considered. Our 3D FEM model is able to represent either the whole construction, or half of it, following longitudinal symmetry; in that case, the cut is a longitudinal plane that presents mirror symmetry for the magnetic

component of the field, and it is specified by a *perfect magnetic conductor* type boundary condition (applied to the magnetic field strength  $\mathbf{H}$ )

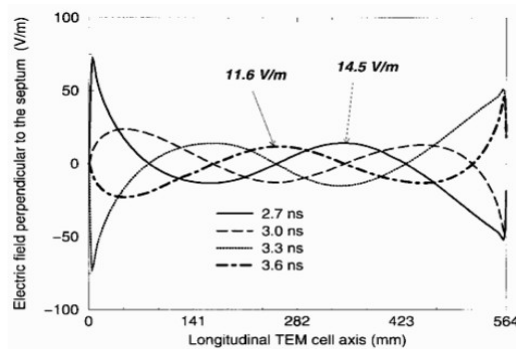
$$\mathbf{n} \times \mathbf{H} = 0. \quad (4)$$

In the case of the cell loaded with a biological sample, the symmetry conditions may not apply in the same way; the sample could be positioned either on the septum or on the bottom of the cell and possible asymmetric shape or positioning of the dish containing the biological material would cause dissymmetry.

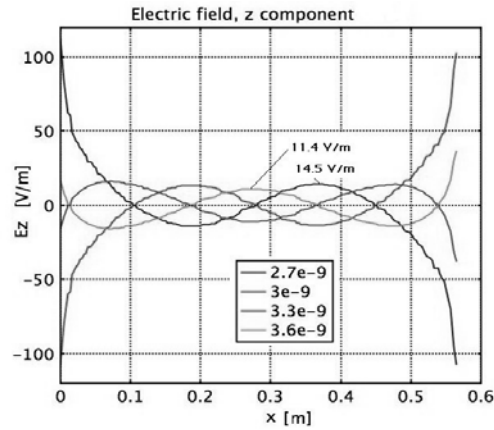
## 2.2. THEORETICAL VALIDATION OF THE MODEL

Prior to the evaluation performed on the cell characteristics, several tests and validation procedures were necessary in order to verify and gain control of the numerical model. First, a FEM model (similar to the above description) was created with the geometry and dimensions introduced by paper [2], with the goal of replicating the results obtained there (with the FDTD numerical method). The electric field strength distribution and the *voltage standing wave ratio* (VSWR) in the unloaded cell, as well as the SAR distribution in a rectangular enclosure filled with biologic material, are the results referred in the cited work and verified by our 3D FEM model, leading to a very good agreement.

VSWR is computed by our 3D FEM model from the snapshots of the  $E_z$ -component of the electric field strength, taken one-quarter cycle apart in time, along the longitudinal axis of the cell and 4 mm distance above the septum (the method is indicated in the referred paper). The working frequency is 0.837 GHz, as considered in [2]. VSWR is defined as the ratio between the higher and the lower amplitudes. Fig. 2 shows the comparison we have made between our results and those presented in the cited paper. The similarity shows to be fully satisfactory and was also used as a criterion for numerical accuracy tests and settings.



a) graph cropped from paper [2], VSWR = 1.25



b) graph obtained with our 3D FEM model, VSWR = 1.27

Fig. 2 – Line graphs of the  $E_z$ -component of the electric field strength on the direction of wave propagation ( $x$ , or the longitudinal axis), 4 mm above the septum; the curves are one quarter cycle apart in time and allow the computation of VSWR.

In the same manner we performed a second theoretical validation of our 3D FEM model, going further with the comparison with results presented in paper [2]. The SAR distribution inside a rectangular glass dish containing biological material and placed above the septum was replicated with our 3D FEM model, complying with the same exposure conditions (dish geometry, material properties, frequency, injected power). Defined as the rate of incremental energy  $dW$  absorbed by (or dissipated in) an incremental mass  $dm$  contained in a volume  $dV$  of a given density  $\rho$ , the quantity SAR could be expressed, at any location inside the body exposed to EMF, with the aid of the electric power density, that depends on the r.m.s. value of the electric field strength  $E$ , as follows

$$\text{SAR} = \frac{d}{dt} \left( \frac{dW}{dm} \right) = \frac{d}{dt} \left( \frac{dW}{\rho dV} \right) = \frac{\sigma E^2}{\rho}. \quad (5)$$

Fig. 3 displays a reasonable similarity of data from the referred work, against corresponding outputs of the 3D FEM model validated here.

The comparison of results opens the opportunity for a parallel evaluation of the numerical methods involved. Both models perform well to EMF computation inside the TEM cell, but they are complementary in advantages and suitability. The FDTD method is more common for high frequency EMF computation and it makes use of efficient solver algorithms that are adapted to both general variable and harmonic working conditions, but the stepping approximation of boundaries with uniform rectangular elements could alter the shape of the objects, the precise

identification of subdomains and consequently the accuracy of the solution. On the other side, FEM provides a much finer approximation of the geometries with its tetrahedral elements and the adaptive meshing capabilities allow for accuracy in geometrical representation as much as for economical control of the solving precision in specific regions of interest.

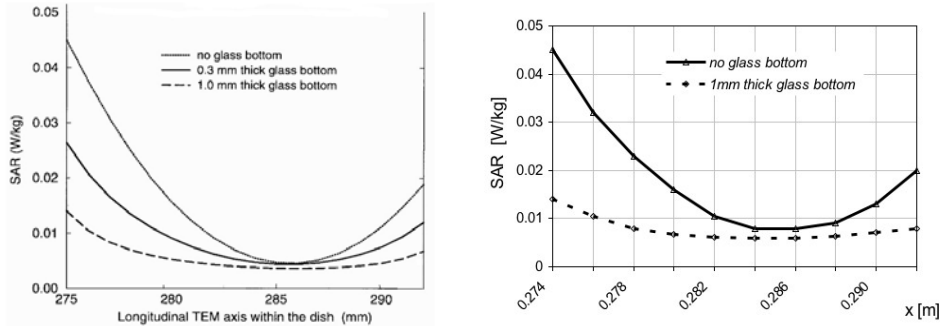


Fig. 3 – SAR distribution inside a glass dish filled with biologic material. Three cases were considered in paper [2] – the bottom of the glass dish has alternatively the thickness 0 mm, 0.3 mm and 1 mm (left graph), while we replicated two cases – 0 mm and 1 mm (right graph). The plots are taken along the longitudinal direction ( $x$  axis), at half the height of the dish (837 MHz, 10 mW).

### 2.3. EXPERIMENTAL VALIDATION OF THE MODEL

The 3D FEM numerical model of the cell presented above was also validated through experimental tests pointing to the *scattering parameters* and VSWR. A set of measurements was made for the  $S$ -parameters determination by using a PNA-L network analyzer model N5230A-Agilent (10 MHz to 40 GHz) connected to the TEM cell feeding port, with the end port connected to a matched impedance of 50 ohm. The measured *input port voltage reflection coefficient*  $S_{11}$  was used to estimate VSWR

$$\text{VSWR} = (1 + |S_{11}|) / (1 - |S_{11}|). \quad (6)$$

We compared the VSWR experimental and numerical results for several working frequencies within the range (0.8 ... 1.8) GHz. Both experimental and numerical tests were performed on the TEM cell analyzed in our work (model IFI CC 104) specified in Fig. 1 and Table 1. The results of this validation stage is illustrated by Fig. 4, which shows the measured and computed VSWR values; the percentage differences fall within a 25% interval, considered here as an acceptable tolerance limit.

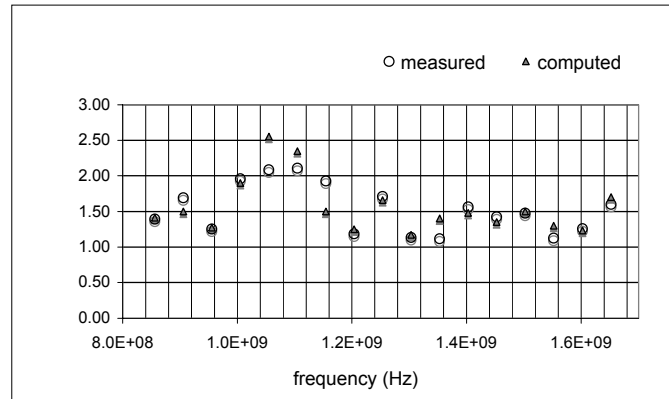


Fig. 4 – VSWR in the TEM cell (model IFI CC 104) – measured *versus* computed values.

### 3. ASSESSMENT OF THE ELECTRIC FIELD UNIFORMITY

The presented TEM cell (model IFI CC 104, Fig. 1 and Table 1) was primarily evaluated from the perspective of impedance matching and inner electric field uniformity. A preliminary analysis, based on the expressions given in [1], determines the characteristic impedance of the cell  $Z_0 = 51.45 \Omega$  and the cut-off frequency  $f_c = 0.333$  GHz for the first order propagating mode  $TE_{10}$ , which sets the superior limit for TEM wave-mode propagation. However, the dosimetric investigation that we need to perform with the TEM cell requires higher frequencies exposure of the biological samples. This is the reason for evaluation the cell characteristics in the frequency range of (0.8 ... 1.8) GHz.

The technical specification of the cell recommends to virtually enclose the exposed sample in a rectangular test volume (RTV) located either on the septum or on the metallic bottom of the cell, in the central area; its dimensions should not exceed one third of the volume between the septum and the walls of the TEM cell;  $\frac{1}{3}A \times \frac{1}{3}C \times \frac{1}{3}b_2$  represent  $150 \times 150 \times 75$  (in mm) in the  $x$ ,  $y$ ,  $z$  directions. Our study primarily investigates the uniformity of the time harmonic electric field in the RTV, at the working frequency of 0.9 GHz, which is important for a dosimetric analysis focused on the study of MW bio-effects, observed on several samples of cereal seeds, prepared for EMF exposure in the RTV.

The EMF solution shows that only the  $E_z$  component of the electric field (component of  $\mathbf{E}$  along the  $z$  axis, perpendicular to the septum and to the propagation direction) is significant within the RTV. This assertion is based on the electric field spectrum-plot visualization and on a quantitative estimate of  $E_x$ ,  $E_y$  and  $E_z$  components of the electric field strength in the RTV. Fig. 5 shows the  $E_z$

spectrum in two slices: a cross-section perpendicular to the longitudinal axis of the cell (left) and a longitudinal plane of symmetry (right); the spectrum displayed here is limited to values in the range  $\pm 100$  V/m; consequently, the region surrounding the septum margins is eliminated due to the extreme values caused by the discontinuities at the edges. In such conditions, the area of quasi-uniformity of the  $E_z$  field is better evidenced by the almost uniform color above the septum, in the central region of the cell. It coincides roughly with the RTV defined earlier.

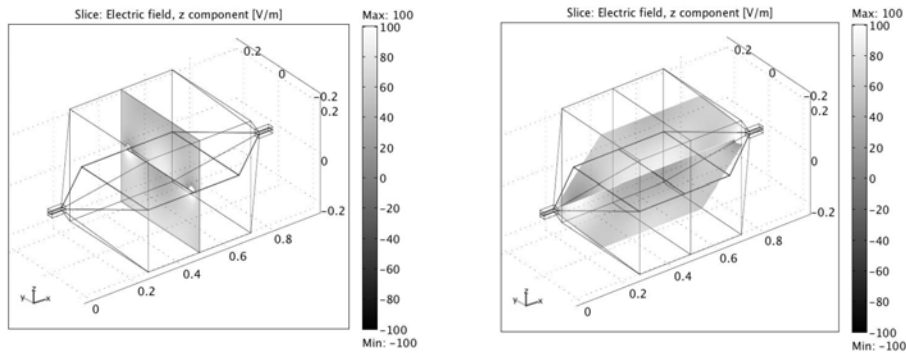


Fig. 5 –  $E_z$ -field spectrum for the uniformity analysis ( $P_{in} = 0.4$  W,  $f = 0.9$  GHz).

The three  $E$ -field components were compared in the RTV region, and Fig. 6 shows  $E_x$ ,  $E_y$  and  $E_z$  along an axis parallel to the septum, at 25 mm height, in the transversal (left) and correspondingly longitudinal (right) slices, defined above; the  $E_x$  and  $E_y$  components become more important against  $E_z$  component as the distance from the septum grows.

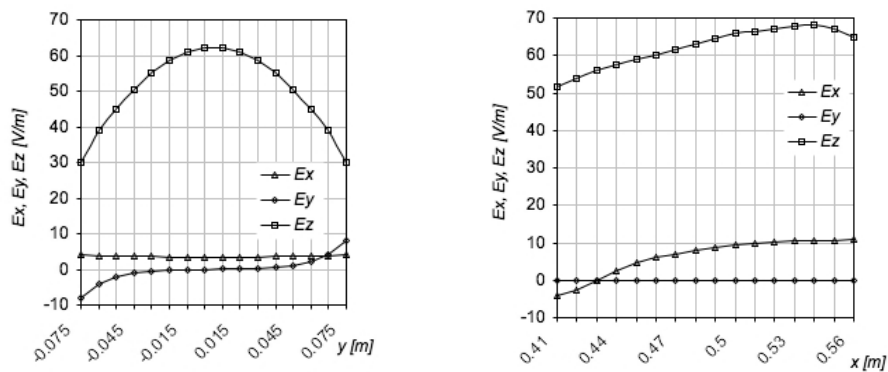


Fig. 6 –  $E_x$ ,  $E_y$ ,  $E_z$  – components of the electric field strength at 25 mm above the septum in the slices displayed by Fig. 5 ( $P_{in} = 0.4$  W,  $f = 0.9$  GHz).

For a quantitative assessment of the field uniformity, Fig. 7 shows the distribution of  $E_z$  – component inside the RTV region, along a centered transversal  $y$ -axis (left) and along a centered longitudinal  $x$ -axis (right) at three heights ( $h_1 = 60$  mm,  $h_2 = 40$  mm,  $h_3 = 20$  mm, measured from the surface of the septum). The uniformity of the electric field is evaluated here with regard to the average value of  $E_z$  inside the RTV ( $E_{z, med} = 51$  V/m at the inward power of 0.4 W and all  $E_z$  values are rated to  $E_{z, med}$ ).

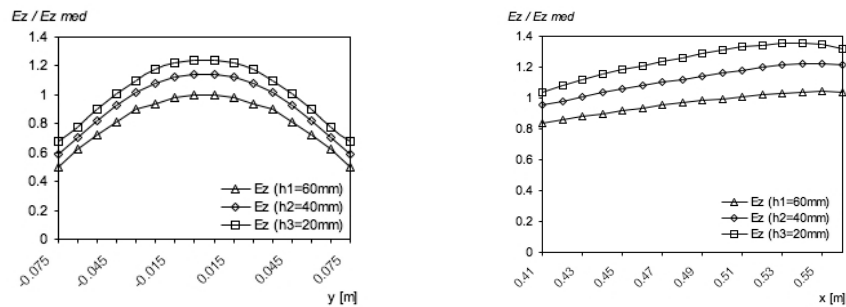


Fig. 7 –  $E_z$ -component distribution inside the RTV, at three heights, along a transversal axis (left) and a longitudinal axis (right), when the RTV is placed on the septum ( $f = 0.9$  GHz).

A similar analysis is performed when the RTV is placed on the bottom of the cell (the TEM cell is reversed from its position in Fig. 1, as will probably be the setting in our testing program). Fig. 8 shows similar  $E_z$  distributions as Fig. 7; the three heights are measured here from the bottom (conductive wall) of the TEM cell and  $E_{z, med} = 29$  V/m inside the RTV.

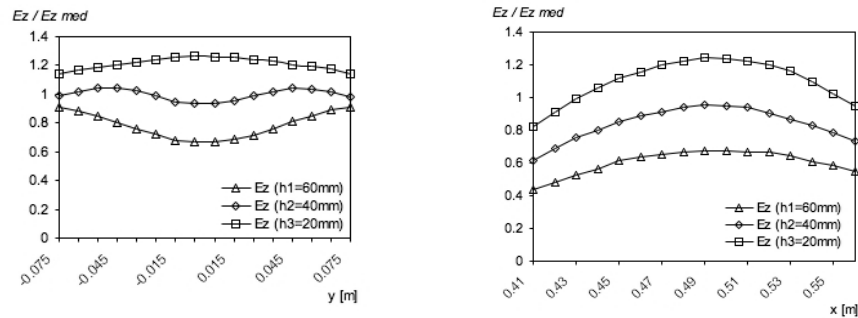


Fig. 8 –  $E_z$ -component distribution inside the RTV, at three heights, along a transversal axis (left) and a longitudinal axis (right), when the RTV is placed on the bottom of the cell ( $f = 0.9$  GHz).

One could observe that  $E_z$  distribution inside the RTV leads, for both settings, to values that may differ from  $E_{z, med}$  with up to  $\pm 40\%$ . The uniformity of the  $E_z$ -field proves to be comparable for both considered cases; however,  $E_{z, med}$  is higher

in the region above the septum. The choice of using either the septum, or the bottom of the cell, as the support surface for the exposed sample becomes a matter of convenience, related to the layout of the experiment; dimensions and shape of the culture dish or biological sample may become sometimes an important condition.

#### 4. CONCLUSIONS

We presented here the characteristics, validation and preliminary assessment of a numerical model that simulates a TEM cell, which is available for a dosimetric investigation program performed on biological samples exposed to MW. The numerical 3D FEM model of the cell, implemented in COMSOL Multiphysics, is designed as a complementary research tool available in parallel with in situ measurements. The accuracy and completeness of the numerical model is evaluated through several tests that imply validation against data published in the literature and against experimental results. The evaluation of scattering parameters and the assessment of electric field uniformity in the central region used for testing provide data useful for the design of the dosimetric study. When a trustful model is on hand, numerical simulation gives access to a much more comprehensive volume of information and makes it possible to determine data not available by experiment.

**Acknowledgements.** The work presented here is supported through the research CEEX projects code PC-D06-PT10-464/2005 and PC-D11-PT14-258/2005 and CNCSIS grant 357/2007, funded by the Romanian Ministry of Education and Research.

*Received on 25 January 2008*

#### REFERENCES

1. M. L. Crawford, J. L. Workman, C. L. Thomas, *Expanding the Bandwidth of TEM Cells for EMC Measurements*, IEEE Trans. on EMC, **20**, 3, pp. 368–375 (1978).
2. M. Popovic, S. C. Hagness, A. Taflove, *Finite-Difference Time-Domain Analysis of a Complete Transverse Electromagnetic Cell Loaded with Liquid Biological Media in Culture Dishes*, IEEE Trans. on BME, **45**, 8, pp. 1067–1076 (1998).
3. K. Malaric, J. Bartolic, *Design of a TEM-Cell with Increased Usable Test Area*, Turk. J. Elec. Engin., **11**, 2, pp. 143–154 (2003).
4. O. Franek, V. Navratil, Z. Raida, *Analysis of Gigahertz TEM Cell using Finite-Difference Time-Domain (FDTD) Method*, 13th International Conference Radioelektronika, Czech Rep, 2003.
5. M. M. G. D'Amico, *Loaded TEM Cell Versus Free Space: Comparison of the E-Fields Inside Dielectric Spherical Objects*, IEEE Trans. on EMC, **41**, 2, pp. 158–160 (1999).
6. Mihaela Morega, Simona Miclăuș, *Electromagnetic Environment Generated in a TEM Cell for Biological Dosimetry Applications*, International Symposium on Electromagnetic Fields, ISEF 2007, Prague, Czech Rep., Proceedings ISBN: 978-80-01-03784-3 (2007).
7. \* \* \*, COMSOL Multiphysics® 3.3a, copyright © 1994–2007 by COMSOL AB.